

RESEARCH ARTICLE

Deriving Design Rules for Personalization of Soft Rehabilitation Gloves

SHOTA KOKUBU¹, REIJI NISHIMURA², AND WENWEI YU^{1,3}, (Member, IEEE)¹Graduate School of Science and Engineering, Chiba University, Chiba 263-8522, Japan²Department of Plastic and Reconstructive Surgery, The Jikei University School of Medicine, Tokyo 105-8461, Japan³Center for Frontier Medical Engineering, Chiba University, Chiba 263-8522, Japan

Corresponding author: Wenwei Yu (yuwill@faculty.chiba-u.jp)

This work was supported in part by the Japanese Society for the Promotion of Science KAKENHI under Grant JP23KJ0307, and Grant JP22H03450.

ABSTRACT Soft actuators developed for hand rehabilitation show promise, but their practical application requires addressing individual differences and establishing suitable design rules. While joint modular soft actuators offer flexibility for diverse hand dimensions, existing performance validations have only examined a limited number of actuator sizes and neglected crucial factors like joint alignment. Customization efforts have lacked standardization, relying on a trial-and-error approach. Therefore, this study systematically evaluates the impact of actuator design parameters (size and mounting position) on joint range of motion (ROM) and torque, proposing novel design rules based on linear optimization. Experimental assessments, conducted on dummy fingers emulating human biomechanics, provide profound insights into the intricate interplay of design parameters and support performance. The findings strongly advocate maintaining a reference position for stable support, irrespective of actuator size, emphasizing the need to align the actuator with the joint center. The proposed design rules incorporate user-specific finger information, offering customized design rules. Proportionate actuator lengths to single-phalangeal length (PsPL), Proportionate actuator lengths to multi-phalangeal length (PmPL), Proportionate actuator lengths to Range of Motion (PROM), and the Traditional Method are systematically compared. Assistive performances (ROM and torque) and trajectory analysis reveal that the PsPL-designed actuator exhibits the most stable and natural assistive performance. This study emphasizes the importance of understanding actuator deformations for personalized adaptation, providing valuable insights for advancements in assistive and rehabilitative technologies.

INDEX TERMS Soft robotics, soft actuator, hand rehabilitation, finger-motion assistance, personalization, individual differences, design rules.

I. INTRODUCTION

Until now, many different types of wearable devices have been developed to assist in hand rehabilitation, and in recent years, individual differences and their adaptations have begun to be recognized as important design factors, in addition to the function of motor assistance [1], [2], [3]. In addition to rehabilitation patients, there are individual differences in the hands depending on age, sex, and the presence or absence of paralytic symptoms. For example, they are typified by the hand finger size (length dimensions), finger joint range of

motion (ROM), and joint stiffness. According to a survey of finger dimensions in the Japanese population conducted by the Research Center for Human Life Engineering, the average length from the proximal end of the metacarpal bone to the fingertip varies by 13.7 mm between adult men and women, with age-related differences being more pronounced [4]. Orthopedic and surgical studies of the hand have also reported that finger joint ROM is not constant, even in healthy groups, and that some rehabilitation patients have restricted ROM [5], [6]. Increased joint stiffness is often observed in the hands of patients presenting with paralytic symptoms. Because the degree of these factors varies with an individual's medical condition, the assistance required varies

The associate editor coordinating the review of this manuscript and approving it for publication was Tao Wang¹.

from patient to patient. While a given joint ROM and stiffness can be addressed by controlling the output of the device, the proper design of an individualized device concerning size and joint alignment is required. Therefore, personalized design is an important step toward the practical application of rehabilitation devices.

Soft actuator-based rehabilitation devices are promising in terms of personalization. Pneu-net and fiber-reinforced soft actuators are typical molded elastomeric actuators used in hand rehabilitation [7], [8], [9], [10], [11]. They are designed with a chamber structure inside the soft actuator and fiber wrapping around the outer circumference to enable bending and twisting in specific directions [9], [11], [12], [13]. In general, soft actuators are considered potentially safer and more capable of absorbing individual differences than traditional rehabilitation devices with rigid systems because of their higher viscoelasticity and adaptability. In particular, it has been claimed that they can be adjusted and produced to fit the fingers of a user, especially in terms of size [1], [14], [15]. However, the adjustment process involved measuring the finger length of the user and remaking the mold from scratch to mold the soft actuator. This method is not very fast, and any change in the length of the soft actuator can unintentionally affect the assistive performance. For example, a soft actuator tailored for a person with short fingers may not function as well as an actuator of normal length. In addition, such actuators may not provide a sufficient angle or force for proper bending, which leads to improper rehabilitation depending on the joint conditions [3]. It has been reported that a misalignment between the actuator and the hand finger size may cause discomfort and deviation from the natural movement of the hand [15]. Moreover, it has been argued that soft actuators do not require precise joint positioning as rigid devices do [1], [14]. This is because the viscoelasticity and backdrivability of soft actuators are believed to absorb the misalignment of the axis of rotation and unexpected loads [2]. Furthermore, most conventional soft actuators, that is, the whole-finger soft actuator, are designed to cover the entire finger with a single-chambered soft actuator and have not been considered for joint alignment [9], [16]. Therefore, traditional soft actuators are insufficient for individual customization.

To the best of our knowledge, the only approach with potential for low-cost personalization is the modularization of soft actuators. Modularized soft actuators (i.e., joint-modular soft actuators) differ from traditional whole-finger soft actuators in that each joint has an individual actuator. Joint-modular actuators developed for individual adaptations include fabric-based, bellow-based, and fiber-reinforced elastomer-based soft actuators [3], [17], [18], [19], [20]. These joint-modular actuators were interconnected with 3D-printed parts and attached to the patient. Therefore, the process of personalized adjustment requires only modification of the 3D-printed parts and much less time than re-molding the entire actuator. This allows easy customization per module and individual control of the finger joints to assist

in motion. Our previous studies also showed that fiber-reinforced elastomer-based joint-modular actuators exhibit higher flexion performance at lower pneumatic inputs than conventional whole-finger actuators or other types of joint-modular actuators [20]. They also demonstrated a more consistent joint angle and torque support performance than conventional soft actuators for three typical finger sizes [3]. However, all relevant studies, including our previous work, examined only one or several sizes of actuators or hand fingers. In particular, in the case of joint-modular actuators, because each actuator is independent, the size and joint alignment, that is, the mounting position, have not been considered, even though they are more important design parameters.

Although actuator designs for personal adaptation have been proposed, most of them either provide several typical sizes or are based on trial and error to match the lengths of the user's fingers [3], [15], [20]. However, these methods may not provide the best actuator for the individual, or customization may take a long time and be expensive. It is also unclear which actuator design is best for user and personal adaptation. However, there are still no criteria for determining the most important design parameters such as size and mounting position. Therefore, clarifying the effects of each design parameter and defining a design methodology for individual adaptation will help ensure rapid customization and improve the performance of soft rehabilitation gloves in practical applications.

This study investigated the effect of design parameters for personalization on the support performance of a joint-modular actuator, focusing on the size and mounting position. In addition, four design rules based on linear optimization using information from the user's fingers as constraints were proposed and compared. First, a joint-modular actuator based on a fiber-reinforced modular elastomeric actuator was redesigned, and its basic performance was characterized. Subsequently, the effects of different sizes and mounting positions on the performance of the actuator were verified by measuring the joint ROM and torque with a dummy finger. Finally, the effect of personalizable design rules reflecting the results was tested on a dummy finger, and the safety was examined by comparing it with the trajectory of a healthy human hand joint.

II. JOINT MODULAR SOFT ACTUATOR

A. PRINCIPAL DESIGN

The joint-modular soft actuator consists of a silicone body, an internal chamber, an air inlet tube, reinforcement fibers, and connectors at both ends (Fig. 1). Joint-modular actuators can be connected to a 3D-printed connector or spacer. For example, three joint-modular actuators must be connected with connectors or spacers to support the index finger. Joint-modular actuators with different lengths can be fabricated by changing the mold. In addition, connectors and spacers can be fabricated quickly using a 3D printer to match the user's

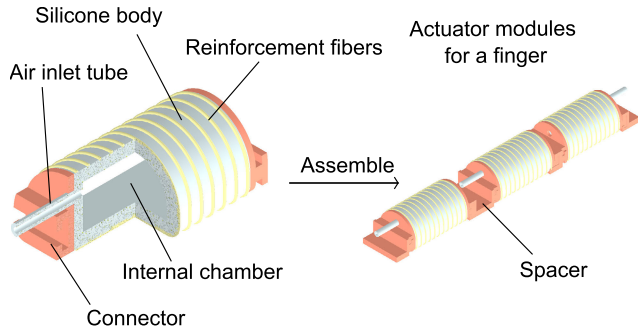


FIGURE 1. Design and assembly method for joint-modular actuators.

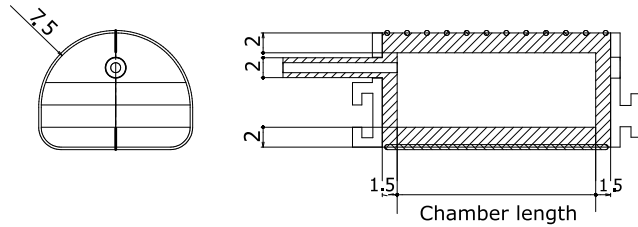


FIGURE 2. CAD drawings: cross sections and dimensions of joint-modular actuator.

hand dimensions. Therefore, the design can be customized to suit the users with minimal effort.

The factors that affect the performance of the joint-modular actuator include the silicone and reinforcement fiber material, and the design of the chamber shape, width, and length. The silicone used to make the actuator was Dragon Skin 10NV (Smooth-On, Inc., US), and the reinforcement fiber was selected as cotton thread (Shinwa Rules Co., Japan). The cross-sectional shape of the actuator internal chamber was determined to be semicircular. Based on the results of previous studies, materials were selected for stable operation of the actuator, and the shape was chosen to maximize the bending performance [8], [9], [21]. The width of the chamber was maximized to fit the average width of the Japanese fingers, and all designs were standardized for comparison [4]. On the other hand, the length of the actuator was chosen to investigate its effect on performance, with 10, 15, 20, 25, and 30 mm as representative test cases (Fig. 2). The difference in lengths chosen as the test cases was ± 5 and 10 mm based on 20 mm, which was designed as the standard size in previous studies [3], [22]. This length can also be modified according to the design rules described in Section II-C.

B. CHARACTERIZATION

Before the relationship between the actuator and fingers can be investigated, it is necessary to determine the characteristics of the actuator relative to its design parameters (length). In several previous studies, the basic performance or characteristics of soft actuators were measured in terms of the bending angle during actuator pressurization [8], [9]. Therefore, this study investigated the bending angles of individual actuators of different sizes. As in previous studies, the bending angle is defined as the angle between the normal vectors of the actuator tip and root edges (Fig. 3) [3].

The bending angle can be measured by reading 2D markers attached to the tip and root of the actuator from the camera images. Joint-modular actuators with chamber sizes of 10, 15, 20, 25, and 30 mm were selected as test cases, as described in Section II-A. The air pressure during the characterization was set to 50, 100, and 150 kPa.

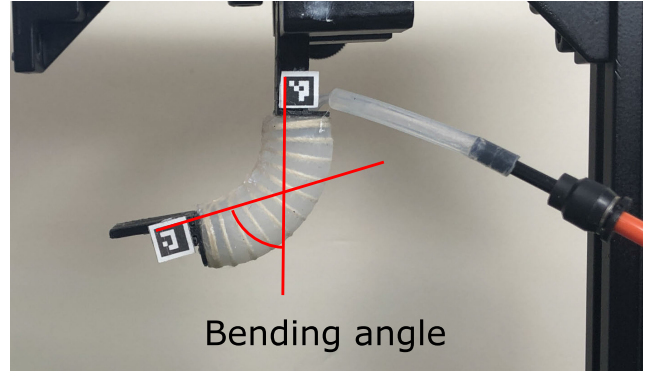


FIGURE 3. Definition of bending angle as an actuator characteristic and its measurement setup.

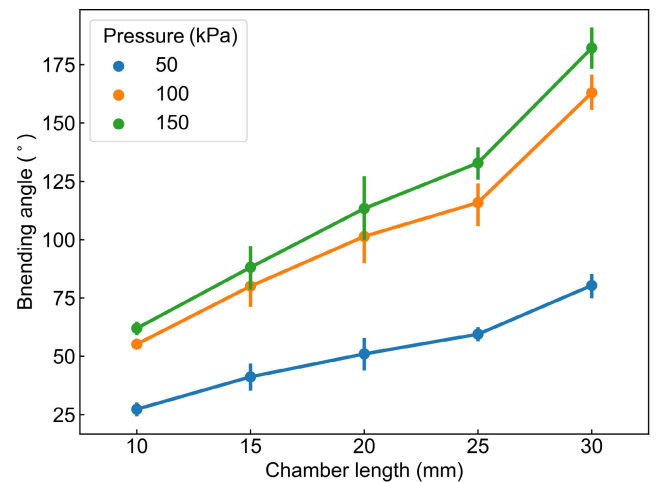


FIGURE 4. Bending angle as chamber-length-dependent function of air pressure.

Fig. 4 shows the relationship between the joint-modular actuator size and the bending properties. The plot shows the average of the three data points, and the error bars show the variance. Under the same experimental air pressure, the actuator’s size increased, and the bending angle also increased. The relationship between the actuator size and bending angle remained consistent across all experimental air pressure conditions. This indicated that the bending performance of the actuator was proportional to its length as a design parameter. This trend is similar to that of a related study, which showed that longer actuators with a specific cross-sectional area and geometry provide better bending performance [8]. The bending angle also increased with the air pressure, similar to the characteristics of soft actuators reported in previous studies [8]. Thus, the joint-modular actuator has the same characteristics as the other actuators,

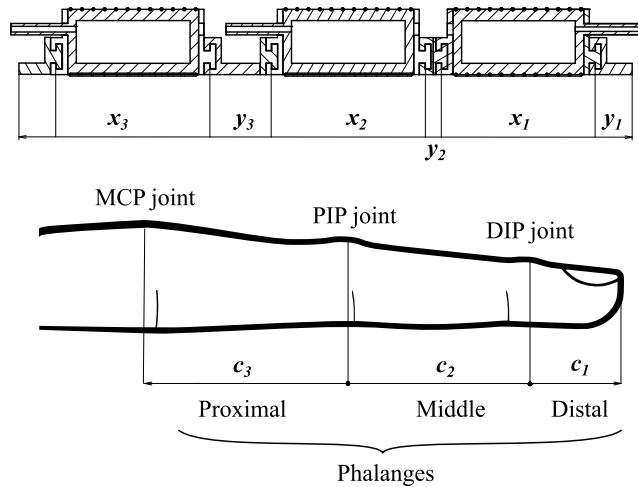


FIGURE 5. Relationship between actuator and finger dimensions in the design rules.

indicating that maximizing the design parameters (length) leads to better bending performance.

C. DESIGN RULES FOR PERSONALIZATION

This study proposes four design rules with constraints based on user-hand information to adapt to individual differences. The characterization shown in Section II-B shows that the larger the length of the actuator, the better the bending performance. Therefore, it is necessary to maximize the length and optimize the overall design to improve the bending performance of the actuator, while adapting to individual differences. Therefore, in this study, the relationship between the length of each joint-modular actuator and the connector or spacer configured to support a single finger is presented as a linear function and considered as an optimization problem to maximize the length of the actuator. The optimization problem is then solved using linear programming with an objective function and constraints based on the user's hand information. The objective function for maximizing the actuator length in linear programming is as follows:

$$\arg \max_{x, y \in [0, \infty)} \sum_{i=1}^3 x_i - y_i \quad (1)$$

where x denotes the actuator length, y the connector length, and the subscripts indicate the corresponding joint positions (Fig. 5). Maximizing the length of the actuator in the limited space above the finger is also synonymous with minimizing the spacer, and Equation 1 was set up to find a unique solution.

A common constraint of linear programming is that the length of each phalanx of the user must match the lengths of the corresponding actuator, connector, or spacer. The common constraint are as follows:

$$c_i = \begin{cases} \frac{x_i}{2} + y_i & (i = 1) \\ \frac{x_{i-1} + x_i}{2} + y_i & (i \geq 2) \end{cases} \quad (2)$$

where c denotes the length of the phalanx, and the subscript denotes the corresponding joint position. This constraint implies that the lengths of the three assembled actuators and spacers match the lengths of the fingers of the user.

The four proposed design rules differ in their constraints, except for Equation 2. The constraints added by the three proposed design rules included the length of each phalanx or joint ROM, which was used as the weight to determine the actuator length. The length of each phalanx or joint ROM is a parameter that has been commonly used in previous studies when designing actuators through trial and error, and it is necessary to verify the effectiveness of these parameters in practice [3], [17]. Therefore, the remaining one rule follows the traditional method and is not weighted to determine the length of each actuator for comparison.

The first rule determines that the actuator length is proportional to the length of the distal phalanx adjacent to a specified joint. This paper describes this rule as "Proportionate actuator lengths to single-phalangeal length (PsPL). The relationship between the size of each actuator and phalangeal length is as follows:

$$\frac{x_1}{c_1} = \frac{x_2}{c_2} = \frac{x_3}{c_3} \quad (3)$$

Each denominator represents the length of the corresponding phalanx, which directly affects the actuator size. The longer the phalanx of the denominator, the larger the actuator size.

The second rule determines the actuator length in proportion to the length of the bilateral phalanges adjacent to a specified joint. This paper describes this rule as "Proportionate actuator lengths to multi-phalangeal length (PmPL). The constraints are almost the same as those for the first rule; however, information on the lengths of the two phalanges is used in the denominator.

$$\frac{x_1}{c_1 + c_2} = \frac{x_2}{c_2 + c_3} = \frac{x_3}{2c_3} \quad (4)$$

As in Equation 3, the longer the phalanges, the larger the actuator size. However, the difference in each actuator length is more moderate than that in equation 3 because of the use of the two phalangeal length information. The rules in Equations 3 and 4, PsPL and PmPL, preferentially design longer actuators at joints with more room for finger length. Therefore, because human phalanges are generally longer in the order of proximal, middle, and distal, the actuators for each joint are also larger in the order of Metacarpophalangeal (MCP), proximal interphalangeal (PIP), and distal interphalangeal (DIP) joints.

The third rule determines the actuator length in proportion to the joint ROM. This rule is described as "Proportionate actuator lengths to ROM (PROM)" in this paper. Unlike the first and second rules, PsPL and PmPL, the ROM of each joint is used as a constraint.

$$\frac{x_1}{d_1} = \frac{x_2}{d_2} = \frac{x_3}{d_3} \quad (5)$$

TABLE 1. Constraint constants used in linear programming for actuator design and the results of deriving each design rule based on them.

		c_1	c_2	c_3	x_1	x_2	x_3	y_1	y_2	y_3
Constraint constants	Finger lengths	20.60	27.10	37.84	-	-	-	-	-	-
Design rule	PsPL	-	-	-	23.41	30.79	43.00	8.90	0	0.95
	PmPL	-	-	-	22.95	31.25	36.42	9.12	0	4.01
	PROM	-	-	-	24.09	30.11	27.10	8.56	0	9.23
	Traditional method	-	-	-	27.10	27.10	27.10	7.05	0	10.74

(mm)

where d indicates the joint ROM, and the subscript indicates the corresponding joint position. Because Ueba et al. reported that the typical joint ROM in healthy subjects is 90, 100, and 80 ° for the MCP, PIP, and DIP joints, respectively, these ROM data were employed in this study [23]. According to this rule, longer actuators are preferentially designed for joints with a greater ROM. Therefore, the actuators for each joint are larger in the order of the PIP, MCP, and DIP joints.

Finally, a rule commonly used in previous studies was suggested for comparison [3], [20]. This design rule uses the same size for all actuators. This rule will be called the “Traditional Method” in this paper. The constraints of this rule are simple, and all the actuator sizes are equalized.

$$x_1 = x_2 = x_3 \quad (6)$$

By combining Equations 4 and 6, the length of the actuator is determined by the length of the shortest phalanx. Subsequently, the connector and spacer lengths are determined based on the size of the actuator.

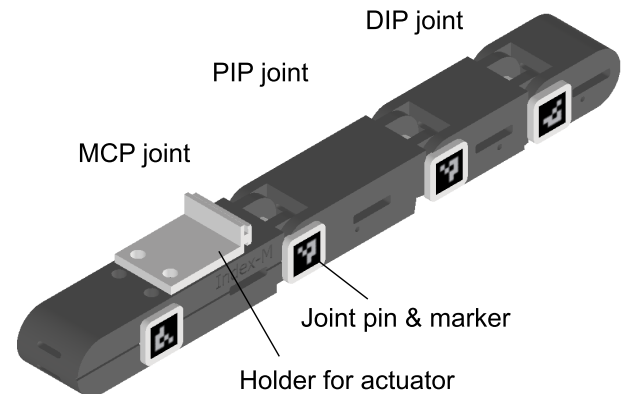
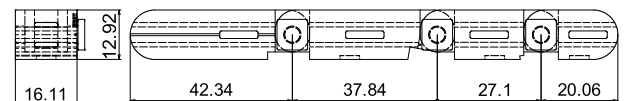
These rules uniquely determine the lengths of all the actuators, connectors, and spacers, thereby facilitating personal customization. In this study, the average finger size of Japanese people was used as a test case for the constraints, and actuators were made based on the respective design rules (Table 1) [4]. The proposed design rules were also compared in terms of support performance, as described in Section III-B.

III. EVALUATIONS

A. VERIFICATION OF EFFECTS OF SIZE AND MOUNTING POSITION

To investigate the effects of different actuator sizes and mounting positions on assistive performance, we mounted each actuator on a dummy finger and measured the joint ROM and torque. ROM and torque are basic measurement items often used to evaluate the support performance of actuators [3], [9], [24], [25]. Therefore, they were selected as indices to investigate the effects of different actuator sizes and mounting positions on the support performance.

Dummy fingers that mimic the structure and biomechanics of a human finger were used for quantitative measurements (Fig. 6). The dummy finger was designed based on the average finger size of Japanese people (Fig. 7) [4]. The dummy fingers have simplified MCP, PIP, and DIP joints, with pin joints and several holes for fixation. Only dummy finger MCP joints and actuators were used as representatives for

**FIGURE 6.** Design of dummy fingers and assembly of components for joint-angle and torque measurement and mounting actuators.**FIGURE 7.** CAD drawings: dimensions of dummy finger.

this measurement. Actuator sizes (chamber lengths) of 10, 15, 20, 25, and 30 mm were chosen, as described in Section II-A. The mounting position was shifted 5 and 10 mm in the distal and proximal directions concerning the center of the joint and actuator (Fig. 8). This joint actuator position criterion has also been commonly used in previous studies [3], [19]. Including that reference position, the mounting positions are -10, -5, 0, 5, and 10 mm, with positive values indicating the distal direction and negative values indicating the proximal direction. For each mounting position, the root of the actuator was fixed to the dummy finger holder using a connector and the tip was banded.

Joint ROM was measured by mounting each actuator on the dummy finger and tracking each joint position with 2D motion capture (Fig. 9) Markers were placed at three locations: the base of the dummy finger, the MCP joint, and the fingertip. The angle of each joint was defined using a marker on the joint and two markers above and below it. To ensure a fair comparison of the actuators, they were banded to dummy fingers at the same relative positions, and the same bands were used. The air pressure range was set to 0-150 kPa for these measurements.

Torque is defined as the product of the force generated during actuator pressurization and the distance between the finger joint and force gauge. The torque at each joint was

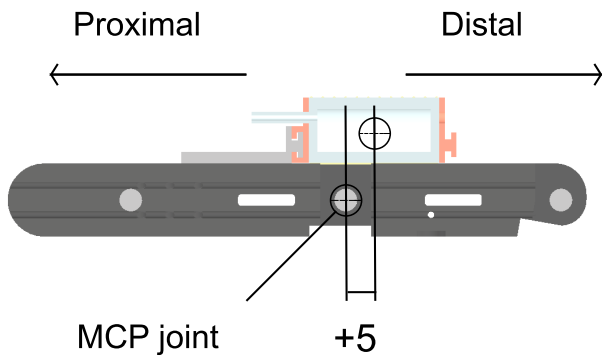


FIGURE 8. Mounting position of the joint-modular actuator to the dummy finger in measurement.

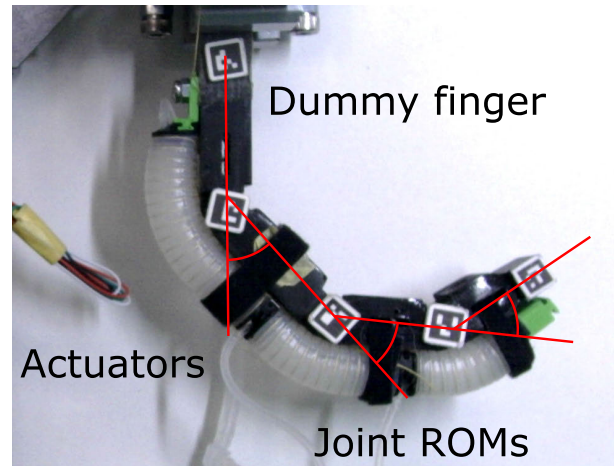


FIGURE 11. Definition of ROM at each joint: all ROM measurements were taken simultaneously at all joints.

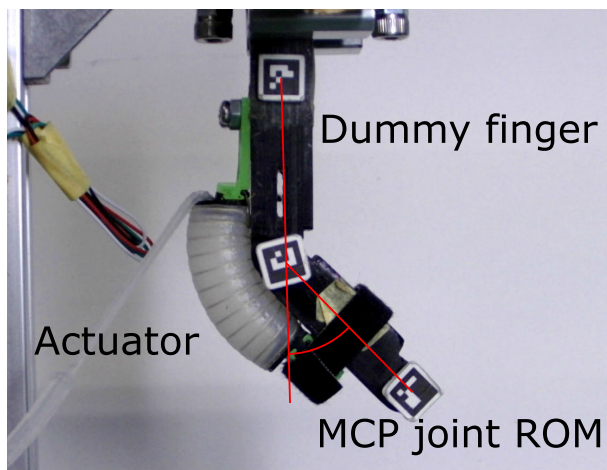


FIGURE 9. Definition and measurement of ROM of MCP joints.

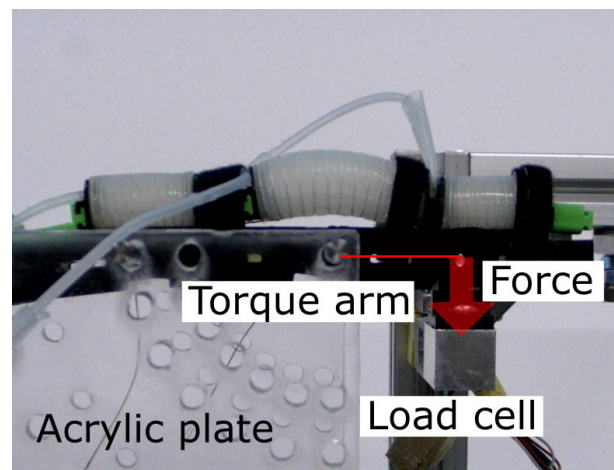


FIGURE 12. Definition of torque at each joint: torque measurements were taken for each joint individually.

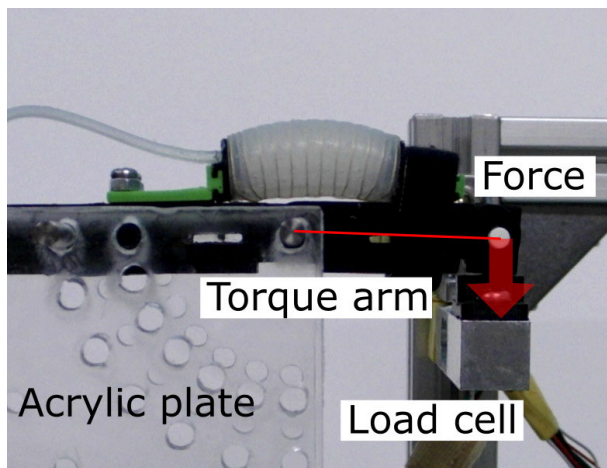


FIGURE 10. Definition and measurement of torque of MCP joints.

measured by fixing one side of the joint to an acrylic plate with a shaft and placing the other side on a force gauge (Fig.10). Similar to the joint ROM measurements, the actuators were banded at the same relative positions using the same band. The air pressure ranged was set for this measurement from 0 to 100 kPa. Thus, there were two

measurement items for 50 measurements: one dummy finger joint, five actuator sizes, and five mounting positions. These measurements were performed at least three times, and the average value was evaluated.

B. COMPARISON OF DESIGN RULES

To investigate the effectiveness of each proposed design method, the joint ROM, torque, and trajectory were measured by mounting the actuators based on each design rule on the dummy fingers. As explained in Section III-A, the joint ROM and torque are fundamental items chosen as benchmarks for support performance. Considering practical situations, joint trajectories were added to the measurement items.

Dummy fingers were used in this measurement, as in the experiment described in Section III-A for the quantitative measures. In this experiment, modular joint actuators assembled for the DIP, PIP, and MCP joints were used for evaluation under more realistic conditions. The actuator design was determined according to the dummy finger dimensions by using the four design rules mentioned in

Section II-C (Table 1). Three actuators were designed and fabricated to support the DIP, PIP, and MCP joints according to each design rule, and connectors and spacers were used as needed. The assembled actuators were banded to dummy fingers at the reference positions using connectors and bands.

Joint ROM was measured in the same manner as in the experiment in Section III-A; however, to measure the ROM of all joints, markers were placed at five locations: the base of the dummy finger, MCP, PIP, DIP joint, and fingertips (Fig. 11). All actuators were pressurized simultaneously, and all joint ROMs were measured. The air pressure ranged was set for this measurement from 0 to 150 kPa.

The torque was also measured in the same manner as in the experiment described in Section III-A, but separately for each joint. This is because the specifications of the measurement setup do not allow the simultaneous measurement of all joints (Fig. 12). The air pressure range was set to 0-100 kPa for these measurements. Thus, two measurement items, three dummy finger joints, and four actuator designs were considered to measure the joint ROM and torque, resulting in a total of 24 measurements.

Trajectories can be measured by reading markers placed on the dummy fingers. Therefore, the setup for the trajectory measurement was the same as that for the ROM measurement (Fig. 11). The actuators were simultaneously pressurized, and the trajectory of each joint of the dummy finger was measured. For these measurements, the pressure range was set from 0 kPa to 150 kPa. These measurements were performed at least three times. The trajectories generated by the actuators mounting the dummy finger were compared with the trajectory data of a human male index finger in total flexion for evaluation [26]. In comparison, the trajectory data of the human index finger were normalized to the length of the dummy finger while maintaining all joint positions and angles.

IV. RESULTS

A. VERIFICATION OF EFFECTS OF SIZE AND MOUNTING POSITION

The measured ROM and torque results were divided into columns for each actuator size and color-coded for each mounting position, as shown in Fig. 13 and 14. The difference in the ROM and torque from the value of the reference mounting position is shown in Fig. 15 and 16 in a similar layout.

The joint ROM increased with increasing air pressure, regardless of the size or mounting position. The maximum ROM tended to increase with the actuator size. These trends are similar to those of a previous study and actuator characterization results [3]. However, for larger sizes (25 and 30 mm), the ROM stabilized at a constant angle of 100 kPa and above. This constant angle was the maximum angle at which the dummy finger could bend. The angle cannot be larger than 90°, which is the maximum angle of the

dummy finger's MCP joint, owing to the specifications of this measurement method.

Differences in ROM according to the mounting position of the actuator on the dummy finger were observed for all sizes, albeit to varying degrees. This difference tended to be greater further away from the reference in the distal or positive directions. The differences were more pronounced for the actuator sizes of 10 mm, 15 mm, and 20 mm. In addition, smaller actuator sizes (10 and 15 mm) sometimes showed a larger ROM than the reference, whereas the others showed either a small error of less than 5° or a smaller ROM than the reference. The difference in ROM for the larger actuator sizes (25 and 30 mm) became drastically smaller at 100 kPa because the ROM for the larger actuator sizes stabilized at a constant angle of 100 kPa and higher.

The torque increased with the air pressure, regardless of the size or mounting position. The maximum torque also tends to increase slightly with an increase in actuator size. The increase is approximately the same trend as in the result of the ROM, but to a lesser degree. This was attributed to the deformation of the actuator and the force escaping to the top, because the torque was measured with the joint fixed.

Torque differences according to the mounting position were shown to be the same extent for all sizes. The torque results at one of the mounting positions are prominent, whereas those at the other mounting positions converge to almost the same values. For instance, with chamber sizes of 10 or 15 mm, the torque showed its peak value at a mounting position of 10 mm. For a chamber size of 20 mm, this occurs at a mounting position of 5 mm, while for chamber sizes of 25 or 30 mm, the maximum torque is observed at the reference position, which is 0 mm.

B. COMPARISON OF DESIGN RULES

The ROM and torque results are divided by columns into values and totals for each joint and color-coded using the design method, as shown in Fig. 17 and 18.

Regardless of the design rule, the joint ROM and torque increased with the air pressure. These trends are similar to those of a previous study and ROM results [3]. The transitions and maximum ROM values vary according to the design rule (Fig. 17 and 19). The traditional method showed the largest ROM for the DIP joint, whereas PsPL showed the largest ROM for the PIP and MCP joints. However, the difference in the maximum ROM for each design rule also differed by joint, especially in the DIP joint, where the difference was smaller than that in the other joints. The actuator length differences for each design rule also varied by joint, and the differences were particularly small for the DIP joints. The total ROM of each joint was larger in the order of PsPL, PmPL, traditional method, and PROM, the value of which is 201°, 194°, 180°, and 164°, respectively. The maximum difference in the total values of ROMs according to the design rule was approximately 40°.

The torque transitions and maximum values differed depending on the design rule, and the differences were

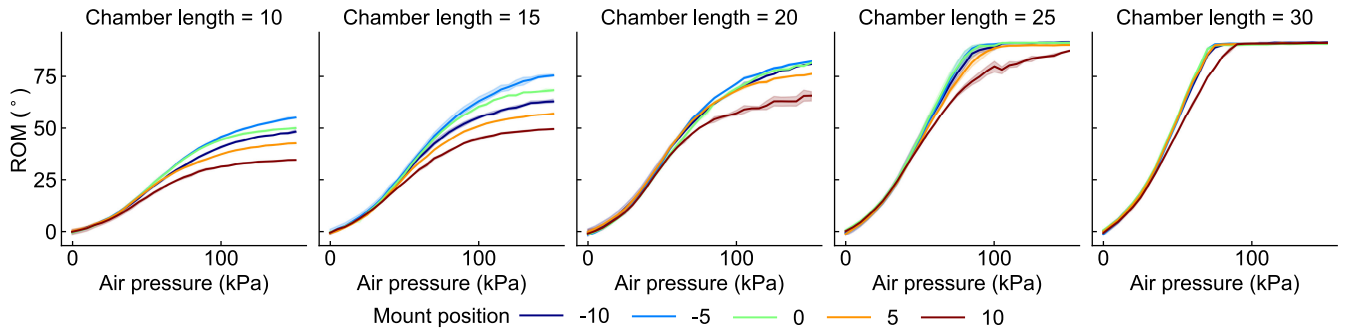


FIGURE 13. Effect of actuator size and mounting position on ROM of MCP joints.

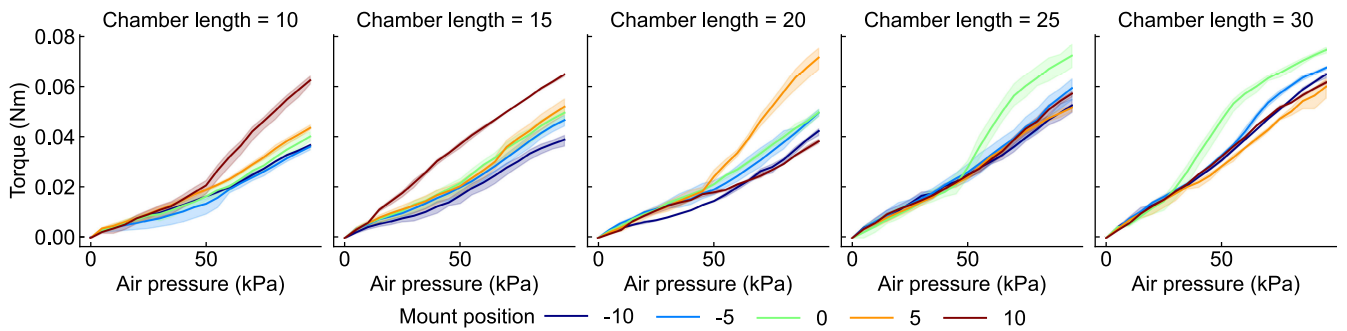


FIGURE 14. Effect of actuator size and mounting position on torque of MCP joints.

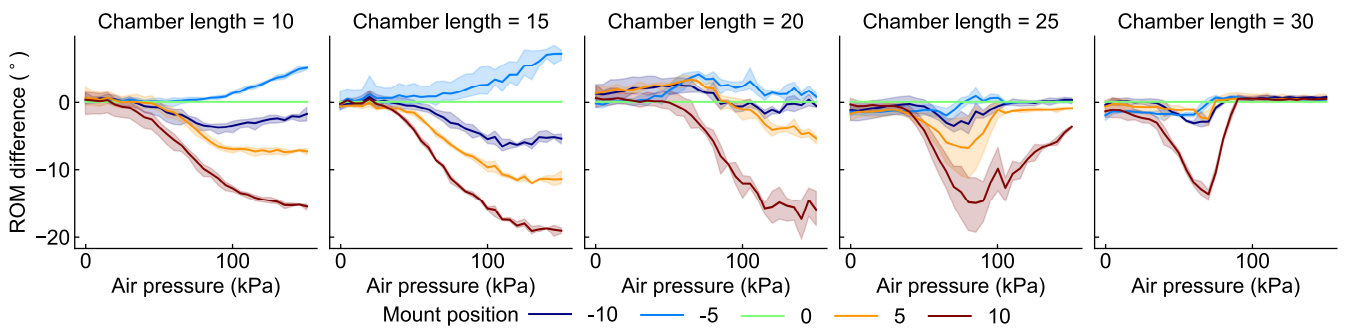


FIGURE 15. Difference in ROM of MCP joints from reference position.

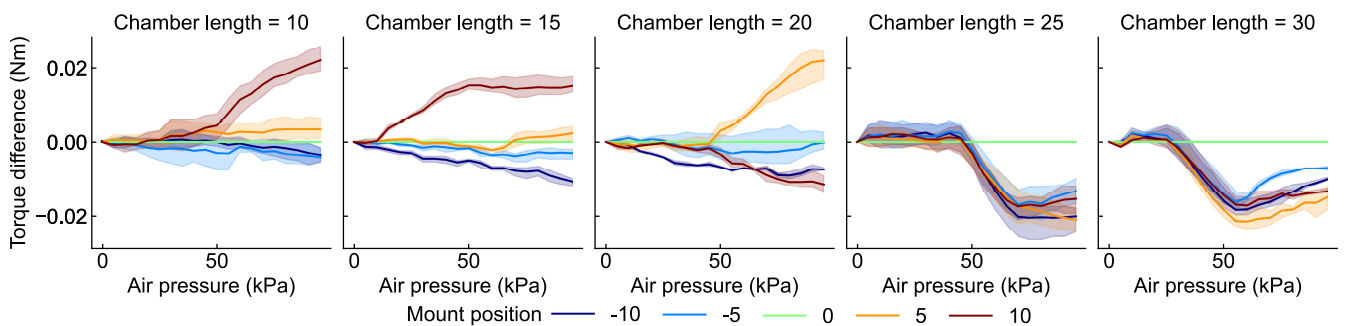


FIGURE 16. Difference in torque of MCP joints from reference position.

particularly small for the DIP joints(Fig.18 and 20). By contrast, the PsPL design rule showed a higher torque for all joints. The maximum total torque for each joint was

larger in the order of PsPL, PmPL, traditional method, and PROM, the value of which is 0.14, 0.01, 0.09, and 0.08 Nm, respectively. The maximum difference in the total

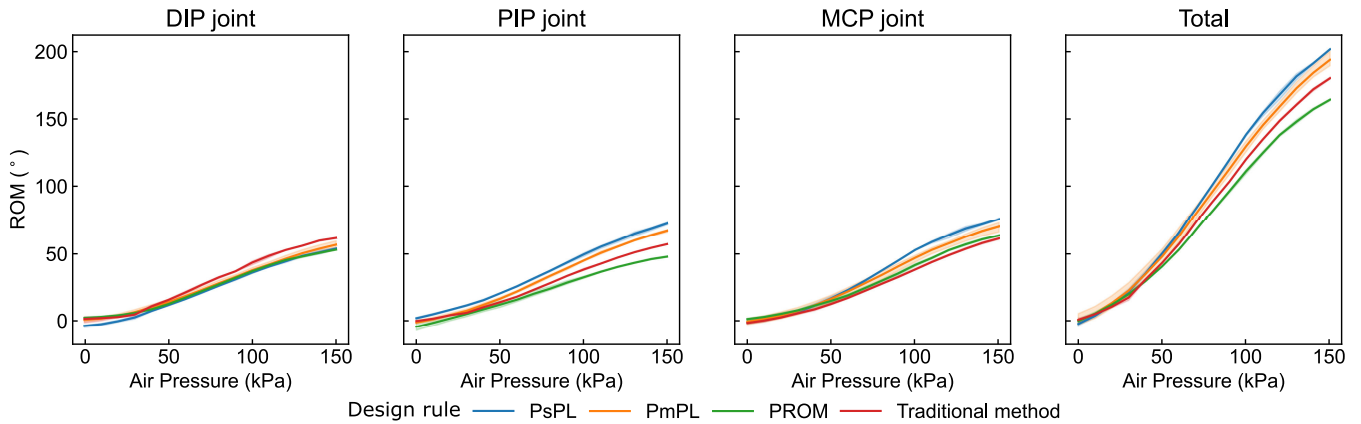


FIGURE 17. Transition of ROM for each joint; comparison of design rules.

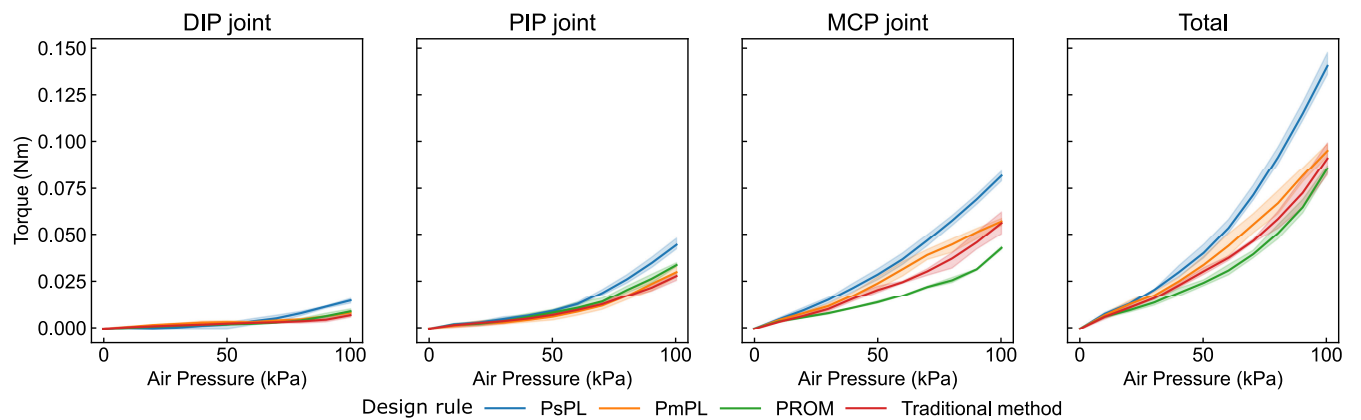


FIGURE 18. Torque transition for each joint; comparison of design rules.

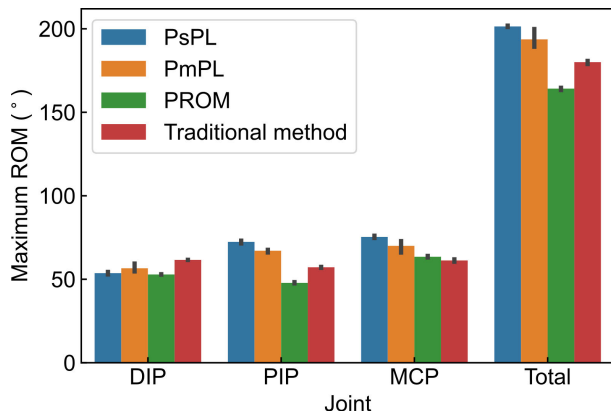


FIGURE 19. Maximum ROM per joint by the design rules.

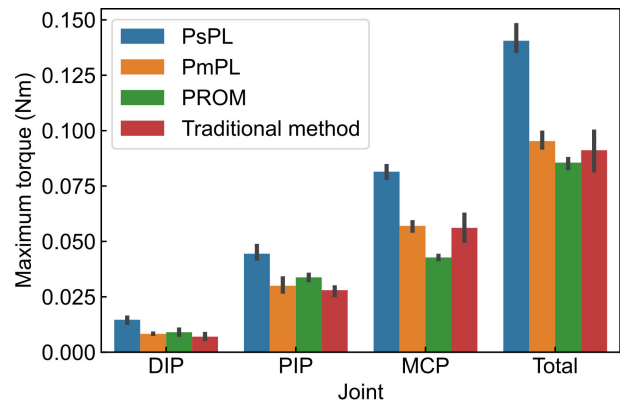


FIGURE 20. Maximum torque per joint by the design rules.

torque values according to the design rule was approximately 0.05 Nm.

The results of the trajectory of the dummy finger with the mounted actuator and the data of the trajectory of the human male index finger are shown in Fig.21. The dots in Fig.21 indicate the positions of each measured joint marker, and the positions of each joint at the initial, intermediate,

and final locations are connected by lines. The shapes of the trajectories generated by the dummy fingers with actuators mounted for each design rule were round and roughly consistent. However, the trajectories of the fingertips differed slightly from those of the other joints, and their final locations differed. The degree of flexion at each location connected by a line shows that PsPL is the most flexed, followed by PmPL and the other design rules. The degree of flexion at

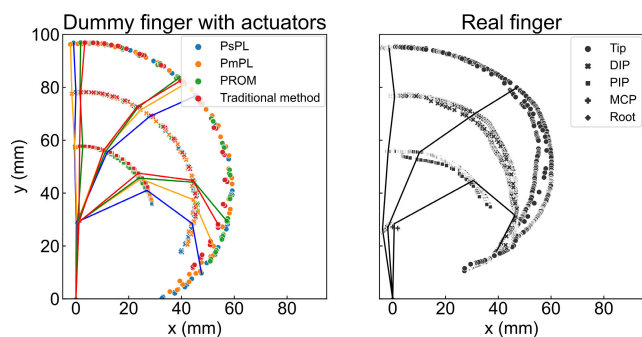


FIGURE 21. Trajectory of dummy fingers and human finger joints.

each location connected by a line also indicated that the PsPL was most consistent with the actual finger.

As described in the literature [27], actual finger trajectories are rounded and resemble isometric curves to some extent. The curves were similar when the actual finger trajectory was compared with the dummy finger trajectory of the joints. However, the fingertip trajectory of the dummy finger exhibited a constant angular curve. Simultaneously, a slight curvature occurred near the final destination of the real finger. The slight curvature near the final location is caused by the fingertip pushing against the soft tissue of the basal phalanx because the PIP joint flexes after the DIP joint has already reached its maximum flexion [26]. Consequently, the final location of the fingertip tip differed between the actual and dummy fingers.

V. DISCUSSION

A. EFFECTS OF SIZE AND MOUNTING POSITION

The effect of the mounting position on the joint ROM and torque was observed for all sizes, but the effect varied slightly. The effect of the mounting position could be caused by a misalignment between the movement trajectory of the actuator and the rotational motion of the joint. When pressurized, the actuator expands and bends in an arc. However, if the actuator is displaced from the center of the joint, it is also displaced from the natural rotational motion of the finger. This effect is particularly noticeable for smaller actuators, and the difference in the ROM or torque from the reference position value tends to be large. This is because even if the misalignment of the mounting position occurs at the same distance, the distance will be relatively large depending on the size of the actuator. For example, a 5 mm misalignment is approximately 17% of the travel for a 30 mm actuator, for a 10 mm actuator, it corresponds to 50% of the travel. Therefore, even soft actuators, particularly those with small sizes, may need to account for misalignment of the mounting position to ensure stable support performance. In addition, even with large actuators, a large misalignment such as 10 mm resulted in a maximum of 10° in the ROM and 0.02 Nm in torque less performance than the maximum value of the reference position. Therefore, the use of an actuator in the reference position is desirable, even for large sizes. This was also evident from the analysis of the response surfaces

with respect to ROM and torque for the actuator design parameters such as chamber size and mounting position (Figure 22, 23).

However, some results showed better ROM or torque than the reference owing to the misalignment of the mounting position. This phenomenon could be due to a shift in the point of action of the force exerted by the actuator on the finger due to the misalignment of the mounting position. Even if the force generated is the same, if the point of action is shifted, the rotation center or torque arm will be different, resulting in a change in the ROM or torque. Considering this phenomenon, intentionally shifting the actuator in the distal or proximal direction for small actuators may lead to better support performance. However, the ROM and torque changes were inversely proportional and occurred only when the mounting position was ± 5 with a small actuator. Specifically, in this situation, extra force (torque) may be applied to the finger even if it is within the defective ROM, or there may be insufficient torque even if there is sufficient ROM. This situation is not only ineffective for rehabilitation but can also be counterproductive. Therefore, based on the results obtained in this study, mounting the actuator in the reference position provided a stable assistive performance. However, the effects of the size and mounting position of the actuator and finger on support performances other than those measured in this study need to be clarified. In particular, careful measurement and observation of the loads on joints and soft tissues exerted by actuators and external loads are necessary to examine safety in real-world applications and will be the focus of future research.

B. DESIGN RULES

The three new actuator design methods and the traditional method showed differences in the results for both the joint ROM and torque at all joints. It is clear from both previous studies and the experiments in this study that the performance varies depending on the length of the actuator [15]. This difference is natural because the actuator length varies depending on the design rules. The difference was significant for the MCP and PIP joints but slight for the DIP joint. This can be attributed to the fact that the differences in the lengths of the actuators fabricated using each design method were larger at the MCP and PIP joints than at the DIP joint. In particular, for the MCP joints, the ROM results were proportional to the designed actuator size. This is consistent with the characterization trends of the actuator bending angles for each size in Section II-B. The total actuator size for each design rule was higher for PsPL, PmPL, PROM, and Traditional, in that order, and the total ROM and torque values were approximately in that order. Therefore, it was shown that maximizing the length of the actuator, which was the premise for the design rule, was effective for improving the supporting performance. The PsPL considered the optimal design rule in this study is proportional to the length of the phalangeal bone, allowing the design of relatively long actuators. The actuator for the DIP joint performed worse with the PsPL than with the

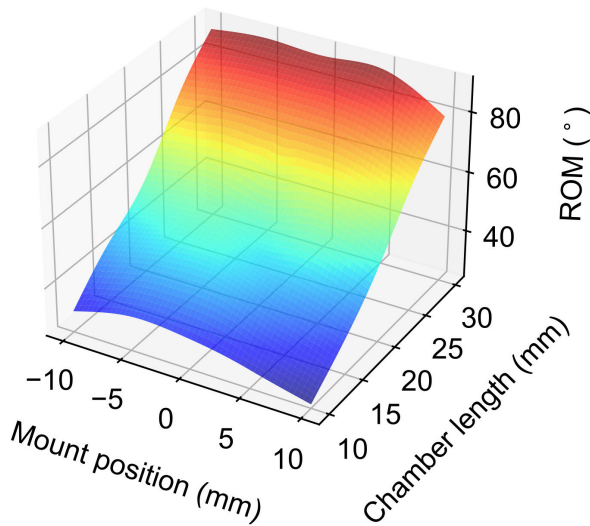


FIGURE 22. ROM response surface of actuator by design parameters.

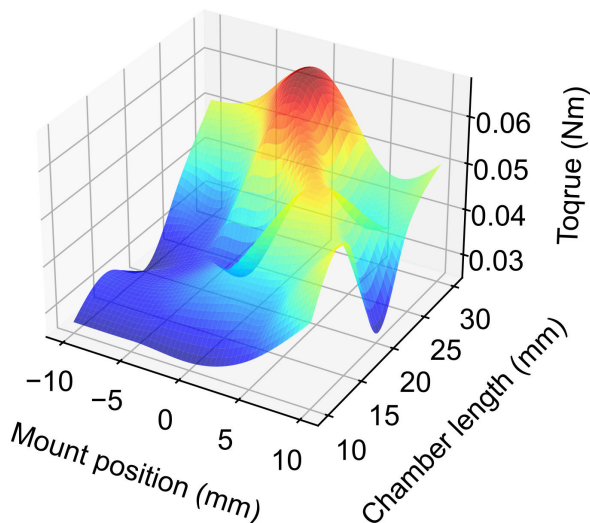


FIGURE 23. Torque response surface of actuator by design parameters.

traditional method, but this may be fine. This can be explained by the fact that the DIP joint is less important than the other joints for grasping and other hand movements, and that the ROM and torque required for flexion are smaller [23], [28]. In addition, given that the MCP joint requires more torque due to contractures in rehabilitation patients, this method is rather convenient [29], [30], [31].

However, the order of actuator size, ROM, and torque magnitude did not always match for joints such as the DIP and PIP joints. For example, the PROM had the largest actuator size in the PIP joint; however, the measured ROM was the smallest. This could be due to the interaction between the fixation method and actuators of each joint. First, the actuator of the MCP joint was screwed through the connector, unlike the other joints, while the other joints were banded in the same relative position with the same band. Furthermore, because all

joints were measured simultaneously, the deformation due to the expansion of the actuators in the other joints affected each other. Therefore, the combination of each actuator design can be related to the overall support performance. Although it is difficult to observe the deformation of actuators and their interactions with each other in actual equipment, this is an important factor in establishing design rules for personal adaptation. Therefore, our future work will investigate the interrelationship between actuators and fingers based on a kinematic model of the actuators.

The trajectories of the dummy finger with the actuators almost matched the actual finger trajectories, except for the fingertip results. In particular, the dummy finger trajectory obtained by the actuator designed using the PsPL rule was the closest to the actual finger trajectory. This indicates that soft actuators fabricated with each design rule can provide natural motion. The fact that the trajectory did not deviate significantly indicated that abnormal joint loading was unlikely to occur. In addition, the deviation of the actuator from the finger, which is thought to lead to the joint strain reported in previous studies, was not observed [3]. However, there are two main reasons for the different fingertip trajectories. One is the size of the actuator and the other is the control method used in the experiment.

The actuators for DIP joints were not designed to be large in most of the design methods proposed in this study. This is because the phalanges near the DIP joint are generally shorter and the range of motion of the DIP joint is smaller. The position of the fingertip depends on the movement angle of the actuator in the DIP joint. Considering that the actuator size affects the bending performance, the design rule may need to be improved to achieve more natural finger motions. However, because the decision of the size of each actuator is a trade-off, careful prioritization is necessary. Furthermore, when considering practical applications, the size of the actuator is constrained by the overall system weight and resource consumption (power, compressed air, etc.), thus multi-objective optimization is preferred.

In the trajectory measurements, the actuators of all joints were controlled to be pressurized simultaneously. Therefore, all joints flexed almost simultaneously during the measurement. However, when total flexion occurs in an actual finger, the order of flexion differs from joint to joint. For example, in a previous study, the DIP joint was flexed to its maximum value before the PIP joint [26]. Therefore, the control method used in this study may have caused differences in the trajectory results for the actual and dummy fingers. However, joint-modular actuators have the potential advantage of being controllable individually. Establishing a control method that follows the actual finger joint flexion sequence could provide a more natural rehabilitation aid.

VI. CONCLUSION

This study systematically investigated the impact of actuator size, mounting position, and design rules on joint-modular

soft actuators for rehabilitation. Misalignment, especially notable in more miniature actuators, affected ROM and torque, emphasizing the importance of maintaining the reference position for stable support.

Among the four design rules proposed in this paper, PsPL (Proportionate actuator lengths to single-phalangeal length) emerged as the most effective, closely mimicking natural finger motions, particularly in enhancing support for joints requiring higher torque, such as the MCP joint.

In conclusion, this research provides valuable insights into the design considerations and operational parameters influencing the efficacy of joint-modular soft actuators, paving the way for advancements in assistive and rehabilitative technologies.

APPENDIX

We have examined response surfaces for Range of Motion (ROM) and torque in relation to actuator size and mounting position, two fundamental parameters influencing bending performance (Figure 22, 23). For ROM, we observed a proportional increase with chamber size, contributing to enhanced bending performance, while the impact of mounting position was relatively minor. Conversely, in torque, chamber size exhibited a significant effect, with notable improvements in bending performance, particularly at the reference position (0 mm). Considering these findings, our design approach emphasizing larger chamber sizes and mounting at the reference position, as advocated in this paper, aligns with sound reasoning.

ACKNOWLEDGMENT

The authors thank Yuxi Lu and Zhongchao Zhou for providing insights into the design of the soft actuator. They would also like to thank Pablo Tortós for attempting to model a soft actuator and finger to investigate the joint strain. They would also like to thank Editage (www.editage.jp) for English language editing.

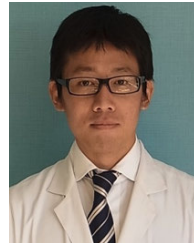
REFERENCES

- [1] H. K. Yap, J. H. Lim, F. Nasrallah, and C.-H. Yeow, "Design and preliminary feasibility study of a soft robotic glove for hand function assistance in stroke survivors," *Frontiers Neurosci.*, vol. 11, pp. 1–14, Oct. 2017.
- [2] K. Shiota, S. Kokubu, T. V. J. Tarvainen, M. Sekine, K. Kita, S. Y. Huang, and W. Yu, "Enhanced Kapandji test evaluation of a soft robotic thumb rehabilitation device by developing a fiber-reinforced elastomer-actuator based 5-digit assist system," *Robot. Auto. Syst.*, vol. 111, pp. 20–30, Jan. 2019.
- [3] S. Kokubu, Y. Wang, P. E. Tortós Vinocour, Y. Lu, S. Huang, R. Nishimura, Y.-H. Hsueh, and W. Yu, "Evaluation of fiber-reinforced modular soft actuators for individualized soft rehabilitation gloves," *Actuators*, vol. 11, no. 3, p. 84, Mar. 2022.
- [4] *Human Hand Dimensions Data for Ergonomic Design*, Res. Inst. Hum. Eng. Quality Life, Osaka, Japan, 2010.
- [5] W. J. Mallon, H. R. Brown, and J. A. Nunley, "Digital ranges of motion: Normal values in young adults," *J. Hand Surgery*, vol. 16, no. 5, pp. 882–887, Sep. 1991.
- [6] S. J. Shaw and M. A. Morris, "The range of motion of the metacarpophalangeal joint of the thumb and its relationship to injury," *J. Hand Surgery*, vol. 17, no. 2, pp. 164–166, Apr. 1992.
- [7] B. Mosadegh, P. Polygerinos, C. Keplinger, S. Wennstedt, R. F. Shepherd, U. Gupta, J. Shim, K. Bertoldi, C. J. Walsh, and G. M. Whitesides, "Pneumatic networks for soft robotics that actuate rapidly," *Adv. Funct. Mater.*, vol. 24, no. 15, pp. 2163–2170, Apr. 2014.
- [8] P. Polygerinos, Z. Wang, J. T. B. Overvelde, K. C. Galloway, R. J. Wood, K. Bertoldi, and C. J. Walsh, "Modeling of soft fiber-reinforced bending actuators," *IEEE Trans. Robot.*, vol. 31, no. 3, pp. 778–789, Jun. 2015.
- [9] T. Tarvainen, J. Fernandez-Vargas, and W. Yu, "New layouts of fiber reinforcements to enable full finger motion assist with pneumatic multi-chamber elastomer actuators," *Actuators*, vol. 7, no. 2, p. 31, Jun. 2018.
- [10] Z. Wang, D. Wang, Y. Zhang, J. Liu, L. Wen, W. Xu, and Y. Zhang, "A three-fingered force feedback glove using fiber-reinforced soft bending actuators," *IEEE Trans. Ind. Electron.*, vol. 67, no. 9, pp. 7681–7690, Sep. 2020.
- [11] K. Ma, Z. Jiang, S. Gao, X. Cao, and F. Xu, "Design and analysis of fiber-reinforced soft actuators for wearable hand rehabilitation device," *IEEE Robot. Autom. Lett.*, vol. 7, no. 3, pp. 6115–6122, Jul. 2022.
- [12] T. Wang, L. Ge, and G. Gu, "Programmable design of soft pneumatic actuators with oblique chambers can generate coupled bending and twisting motions," *Sens. Actuators A, Phys.*, vol. 271, pp. 131–138, Mar. 2018.
- [13] F. Connolly, C. J. Walsh, and K. Bertoldi, "Automatic design of fiber-reinforced soft actuators for trajectory matching," *Proc. Nat. Acad. Sci. USA*, vol. 114, no. 1, pp. 51–56, Jan. 2017.
- [14] H. K. Yap, J. H. Lim, J. C. H. Goh, and C.-H. Yeow, "Design of a soft robotic glove for hand rehabilitation of stroke patients with clenched fist deformity using inflatable plastic actuators," *J. Med. Devices*, vol. 10, no. 4, Dec. 2016.
- [15] P. Polygerinos, K. C. Galloway, E. Savage, M. Herman, K. O. Donnell, and C. J. Walsh, "Soft robotic glove for hand rehabilitation and task specific training," in *Proc. IEEE Int. Conf. Robot. Autom. (ICRA)*, May 2015, pp. 2913–2919.
- [16] T. Tarvainen and W. Yu, "Pneumatic multi-pocket elastomer actuators for metacarpophalangeal joint flexion and abduction-adduction," *Actuators*, vol. 6, no. 3, p. 27, Sep. 2017.
- [17] S.-S. Yun, B. B. Kang, and K.-J. Cho, "Exo-Glove PM: An easily customizable modularized pneumatic assistive glove," *IEEE Robot. Autom. Lett.*, vol. 2, no. 3, pp. 1725–1732, Jul. 2017.
- [18] D. Hu, J. Zhang, Y. Yang, Q. Li, D. Li, and J. Hong, "A novel soft robotic glove with positive-negative pneumatic actuator for hand rehabilitation," in *Proc. IEEE/ASME Int. Conf. Adv. Intell. Mechatronics (AIM)*, Jul. 2020, pp. 1840–1847.
- [19] S. Kokubu and W. Yu, "Developing a hybrid soft mechanism for assisting individualized flexion and extension of finger joints," in *Proc. 42nd Annu. Int. Conf. IEEE Eng. Med. Biol. Soc. (EMBC)*, Jul. 2020, pp. 4873–4877.
- [20] S. Kokubu, P. E. T. Vinocour, and W. Yu, "Development and evaluation of fiber reinforced modular soft actuators and an individualized soft rehabilitation glove," *Robot. Auto. Syst.*, vol. 171, Jan. 2024, Art. no. 104571.
- [21] Y. Wang, S. Kokubu, Z. Zhou, X. Guo, Y.-H. Hsueh, and W. Yu, "Designing soft pneumatic actuators for thumb movements," *IEEE Robot. Autom. Lett.*, vol. 6, no. 4, pp. 8450–8457, Oct. 2021.
- [22] F. Matsunaga, S. Kokubu, P. E. T. Vinocour, M.-T. Ke, Y.-H. Hsueh, S. Y. Huang, J. Gomez-Tames, and W. Yu, "Finger joint stiffness estimation with joint modular soft actuators for hand telerehabilitation," *Robotics*, vol. 12, no. 3, p. 83, Jun. 2023.
- [23] Y. Ueba, *[Hand its Function and Dissection] Te Sono Kinou to Kiabou (in Japanese)*, 4 ed. Tokyo, Japan: Kinpodo, 2006.
- [24] H. K. Yap, P. M. Khin, T. H. Koh, Y. Sun, X. Liang, J. H. Lim, and C.-H. Yeow, "A fully fabric-based bidirectional soft robotic glove for assistance and rehabilitation of hand impaired patients," *IEEE Robot. Autom. Lett.*, vol. 2, no. 3, pp. 1383–1390, Jul. 2017.
- [25] H. K. Yap, F. Sebastian, C. Wiedeman, and C.-H. Yeow, "Design and characterization of low-cost fabric-based flat pneumatic actuators for soft assistive glove application," in *Proc. Int. Conf. Rehabil. Robot. (ICORR)*, Jul. 2017, pp. 1465–1470.
- [26] T. V. J. Tarvainen, W. Yu, and J. Gonzalez, "Development of MorphHand: Design of an underactuated anthropomorphic rubber finger for a prosthetic hand using compliant joints," in *Proc. IEEE Int. Conf. Robot. Biomimetics (ROBIO)*, Dec. 2012, pp. 142–147.
- [27] R. Tubiana, J.-M. Thomine, and E. Mackin, *Examination of the Hand and Wrist*. Boca Raton, FL, USA: CRC Press, Apr. 1998.

- [28] S. Ueki, H. Kawasaki, S. Ito, Y. Nishimoto, M. Abe, T. Aoki, Y. Ishigure, T. Ojika, and T. Mouri, "Development of a hand-assist robot with multi-degrees-of-freedom for rehabilitation therapy," *IEEE/ASME Trans. Mechatronics*, vol. 17, no. 1, pp. 136–146, Feb. 2012.
- [29] D. G. Kamper and W. Z. Rymer, "Quantitative features of the stretch response of extrinsic finger muscles in hemiparetic stroke," *Muscle Nerve*, vol. 23, no. 6, pp. 954–961, Jun. 2000.
- [30] X. Q. Shi, H. L. Heung, Z. Q. Tang, K. Y. Tong, and Z. Li, "Verification of finger joint stiffness estimation method with soft robotic actuator," *Frontiers Bioeng. Biotechnol.*, vol. 8, p. 1479, Dec. 2020.
- [31] R. Prosser, "Splinting in the management of proximal interphalangeal joint flexion contracture," *J. Hand Therapy*, vol. 9, no. 4, pp. 378–386, Oct. 1996.



SHOTA KOKUBU received the B.Eng. and M.Eng. degrees in medical engineering from Chiba University, Japan, in 2019 and 2021, respectively, where he is currently pursuing the Ph.D. degree with the Department of Medical Engineering, Graduate School of Science and Engineering. His research interests include soft rehabilitation devices and human-rehabilitation device interface design and construction.



REIJI NISHIMURA received the M.D. degree from the University of Tsukuba, in 2006, and the Ph.D. degree from The Jikei University, in 2019. He has been an International Visiting Hand Surgery Fellow with the Cleveland Clinic, since 2017. He is currently a Lecturer with the Department of Plastic and Reconstructive Surgery, The Jikei University School of Medicine. He is a Board-Certified Plastic and Hand Surgeon in Japan. His current research interests include hand function, the relationship between the hand and brain, and evolution.



WENWEI YU (Member, IEEE) received the B.Eng. and M.Eng. degrees from Shanghai Jiao Tong University, in 1989 and 1992, respectively, and the Ph.D. degree in system information engineering and the Ph.D. degree in rehabilitation medical science from Hokkaido University, Japan, in 1997 and 2003, respectively. He was an Assistant Professor with the System Information Engineering Department, School of Engineering, Hokkaido University, from 1999 to 2003. In 2003, he was an Exchange Research Fellow with the Center for Neuroscience, University of Alberta, Canada, supported by the Researcher Exchange Program of the Japanese Society for the Promotion of Science (JSPS). Since 2004, he has been an Associate Professor with the Department of Medical System Engineering, School of Engineering, Chiba University, Japan. Since 2006, he has been with the AI Laboratory, University of Zurich, Switzerland, as a Visiting Professor, supported by the JSPS. He has been a Professor, since 2009. He has authored or coauthored more than 150 articles in refereed journals and book chapters, and more than 170 international conference papers. His research interests include neuro-prosthetics, rehabilitation robotics, motor control, and biomedical signal processing. He is also a member of the Robot Society of Japan (RSJ) and the Japanese Society for Medical and Biological Engineering (JSMB).

...